χ_{TS} weight fraction of lignin not in associated complexes
χ_p mole fraction of phenol hydrogen ions

Registry No. Indulin AT, 8068-05-1.

References and Notes

(1) Adler, E. *Wood Sci. Technol.* **1979**, *11*, 169.
(2) Sarkanen, K. V.; Ludwig, C. H. *Lignins*; Wiley: New York, 1971.
(3) Marton, J. *Tappi* **1964**, *47*, 713.
(4) Benko, J. *Tappi* **1964**, *47*, 508.
(5) (a) Yaropolov, N. S.; Tischenko, D. V. *Zh. Prikl. Khim.* **1970**, *43*, 1120. (b) Yaropolov, N. S.; Tischenko, D. V. *Zh. Prikl. Khim.* **1970**, *43*, 1351.
(6) Lindstrom, T. *Colloid Polym. Sci.* **1979**, *257*, 277.
(7) (a) Sarkanen, S.; Teller, D. C.; Hall, J.; McCarthy, J. L. *Macromolecules* **1981**, *14*, 426. (b) Sarkanen, S.; Teller, D. C.; Abramowski, E.; McCarthy, J. L. *Macromolecules* **1982**, *15*, 1098. (c) Sarkanen, S.; Teller, D. C.; Stevens, C. R.; McCarthy, J. L. *Macromolecules* **1984**, *17*, 2588.
(8) Woerner, D. L. Ph.D. Dissertation, University of Washington, 1983.
(9) Woerner, D. L.; McCarthy, J. L. *AIChE Symp. Ser.* **1984**, *80*, 232.
(10) Wilcoxon, J. P.; Schurr, J. M. *Biopolymers* **1983**, *22* (10), 2273.
(11) Brown, A. D.; Saller, B. C. *Quantitative Chemistry*; Prentice Hall: Englewood Cliffs, NJ, 1963.
(12) Hiemenz, P. C. *Principles of Colloid and Surface Chemistry*; Marcel Dekker: New York, 1977.
(13) Marton, J.; Marton, T. *Tappi* **1965**, *48*, 398.

Preferential Surface Adsorption in Miscible Blends of Polystyrene and Poly(vinyl methyl ether)

Qamardeep S. Bhatia†

Department of Chemical Engineering, Princeton University, Princeton, New Jersey 08544

David H. Pan

Xerox Webster Research Center, 800 Phillips Road 0114-39D, Webster, New York 14580

Jeffrey T. Koberstein*

Institute of Materials Science and Department of Chemical Engineering, University of Connecticut, Storrs, Connecticut 06268.

Received November 12, 1987; Revised Manuscript Received January 8, 1988

ABSTRACT: The surface structure and properties of miscible blends of polystyrene (PS) with poly(vinyl methyl ether) (PVME) have been studied as a function of the blend composition and constituent molecular weights. The lower surface tension of the PVME compared to that of PS results in preferential adsorption of PVME at the surface. The surface enrichment of PVME is characterized by measurements of the surface tension as a function of the temperature, accomplished with an automated pendant drop apparatus, and by X-ray photoelectron spectroscopy (XPS). Angle-dependent XPS has been used to determine the surface concentration profiles of the blend constituents. The results of these measurements demonstrate that (1) the PVME surface concentration is elevated substantially from that in the bulk, (2) the integrated surface concentration gradient determined from XPS measurements can be modeled as a $\coth^2[(z/\xi) + \alpha]$ profile where ξ is the screening length, and (3) the degree of surface enrichment depends strongly on the blend composition and molecular weight of the constituents, correlating well with the surface energy difference between PS and PVME.

Introduction

Current technologies frequently employ multiconstituent polymer systems to tailor the material's bulk physical and mechanical properties. Although much emphasis has been placed on understanding the bulk phase relationships and properties of multicomponent polymeric materials, comparatively little is known about their surface structure and properties.

In small-molecule systems, such as metallic alloys[1] and liquid mixtures,[2] it is well-known that the surface composition differs from that of the bulk due to preferential surface adsorption of one constituent. This process is driven, in part, by differences in surface energies and can be expressed classically through the Gibbs adsorption isotherm[3]

$$-d\gamma = \sum_i \Gamma_i \, d\mu_i \qquad (1)$$

where Γ_i is the surface excess ($\Gamma_i \equiv n_i/A$) of component i, dA is the fractional surface area, and μ_i is the chemical potential of species i for n_i moles of that component. From (1) it is apparent that a surface concentration gradient exists in multiconstituent systems where the surface is enriched in the component of lower surface energy (i.e., surface tension γ).

Preferential surface adsorption has been documented by surface tension, contact angle, and X-ray photoelectron spectroscopy (XPS) measurements on several multicomponent polymeric systems. In immiscible binary homopolymer blends, for example, the surface behavior is generally dominated by adsorption of the lower surface energy component.[4,5] This phenomenon also occurs for many blend additives.[6] Since equilibrium bulk thermodynamics favors complete demixing of the two homopolymers, the "equilibrium" surface should be occupied exclusively by the constituent of lower surface energy. In actuality, macroscopic equilibrium is usually not attained in immiscible polymer blends, such that the surface structure obtained is dependent on intrinsic factors such as the relative wettabilities of the two constituents and the degree of phase separation, as well as extrinsic factors including

† Current address: Department of Polymer Science and Engineering, University of Massachusetts, Amherst, MA 01003.

0024-9297/88/2221-2166$01.50/0

the procedure for sample preparation and blend morphology.

A number of investigations of copolymer surfaces have also appeared. Early studies of the surface tensions of block copolymer melts[7,8] illustrated significant surface activity by the sequence of lower surface energy. Surface activity increased with block length, and complete surface coverage by the low surface energy constituent was observed for copolymers of sufficient length. XPS investigations have reported similar results for a number of diblock and triblock copolymer systems.[9-15] Surface enrichment has also been demonstrated in random copolymers of hexamethyl sebacate with dimethylsiloxane and ethylene oxide with propylene oxide.[7] Complete domination of the surface by the lower surface energy constituent does not occur, however, reflecting the influence of configurational constraints that limit migration to the surface.

Block copolymers exhibit similar behavior when added to homopolymers.[16,18] A practical example is the reduction of poly(propylene glycol) surface tension in the manufacture of polyurethane foams.[19] The addition of a few tenths of a percent of certain polyether–polysiloxane block copolymers reduces the surface tension of the blend to that corresponding to pure polysiloxane.

The surface topology of block copolymers has also been investigated by XPS measurements. The results for a number of block copolymers containing dimethylsiloxane (PDMS) sequences[9,13] showed that the surface is comprised of a homogeneous PDMS-rich overlayer, the composition and thickness of which are dependent on the composition and block lengths of the copolymer. Under certain conditions, this overlayer consisted of essentially pure PDMS. In contrast, similar studies on other block copolymer systems have concluded that, although the surface is dominated by the species of lower surface energy, the topology is heterogeneous.[10-12,14,15] That is, the species dominating the surface resided in either lens-shaped, cylindrical, or lamellar microdomains protruding from the surface.

Gaines[20] has attributed the two types of behavior observed for block copolymers to differences in spreading or wetting for the two systems. In the siloxane systems, the surface tension difference between components is large enough to favor surface wetting by the siloxane sequences. In cases where the surface energy difference is small, one sequence cannot wet the other, resulting in a heterogeneous surface as has been found in ethylene oxide block copolymers.[10,11]

More recently, Fredrickson[21] has proposed a theory for surface ordering in block copolymers. Even in the disordered state, block copolymers are shown to possess ordered surfaces with periodic surface composition profiles. The initial theory is derived for systems close to the order–disorder transition (i.e., in the weak segregation limit) and does not consider directly the effects associated with preferential wetting.

There is a large body of experimental data and theory pertaining to the surface properties of polymer solutions, especially concerning their surface tensions.[22-26] The success of these theories in representing the experimental data has been discussed in a recent review.[27] Most polymer–solvent systems show adsorptive behavior for the solute wherein a large initial reduction in surface tension (3–5 mN/m) is seen upon polymer addition. Repulsive behavior (i.e., surface enrichment of solvent) has also been observed for several polymer systems. In this case the surface tension increases almost linearly with polymer concentration until it jumps suddenly to the pure homopolymer value as the polymer concentration approaches unity.

Table I
Characteristics of Specimens

sample designation	M_w	M_w/M_n	source[a]
PS1 (polystyrene)	517	<1.06	3
PS2 (polystyrene)	1200	<1.06	1
PS3 (polystyrene)	2100	<1.10	2
PS4 (polystyrene)	3100	<1.06	1
PS5 (polystyrene)	4000	<1.10	2
PS6 (polystyrene)	9000	<1.04	2
PS7 (polystyrene)	20400	<1.06	2
PS8 (polystyrene)	50000	<1.06	2
PS9 (polystyrene)	110000	<1.06	2
PS10 (polystyrene)	127000	<1.06	1
PVME (poly(vinyl methyl ether))	99000	~2.1	3

[a] 1 = Polymer Laboratories; 2 = Pressure Chemical Co.; 3 = Scientific Polymer Product.

Miscible homopolymer blends are similar to polymer solutions and also exhibit pronounced surface-excess behavior.[7,28,29] Measurements on several oligomeric mixtures reveal that the surface excess is accentuated by increasing the molecular weight. LeGrand and Gaines[29] modeled the surface tension data for compatible oligomers of PDMS and polyisobutylene by a theory that combined the Flory–Huggins lattice model for polymer solutions[30] with the Prigogine–Marechal parallel-layer model.[3] In general, however, careful examination of theories for the surface tensions of miscible blends has been hampered by the lack of knowledge regarding the polymer–polymer interaction parameters.

Recently, Pan and Prest[31] presented initial results of studies on the surface structure of the miscible polymer blend system polystyrene/poly(vinyl methyl ether). X-ray photoelectron spectroscopy was employed to measure both the effective surface composition and surface concentration gradient in the blends. The results demonstrated a pronounced surface enrichment of the poly(vinyl methyl ether). The bulk thermodynamic phase relationships, interaction parameters, and phase-separation mechanisms have already been studied extensively for this miscible blend system.[32-37] The observed phase diagrams exhibit a lower critical solution temperature wherein phase separation occurs upon heating. Miscibility is manifest over a wide range of experimental conditions, making this blend an excellent model system for the study of preferential surface adsorption in polymer systems. In this article, we extend the initial study and report the effects of blend composition and constituent molecular weights on surface enrichment in these miscible polymer blends. The surface structure is characterized by XPS measurements on thin films, while the thermodynamic character of the surface is assessed by determining the surface tensions of blends in the melt state. The results obtained are compared to the predictions of various theories for the surface thermodynamics and structure of polymer solutions.

Experimental Section

Materials and Specimen Preparation. The molecular weights and molecular weight distributions (quoted from the suppliers) of the polystyrene and poly(vinyl methyl ether) specimens are reported in Table I. Prior to usage, the PVME was cleaned by precipitation from toluene solution by the addition of hexane. This procedure was repeated twice and was followed by vacuum drying at 60 °C for a minimum of 1 week.

Blends containing 5, 20, 50, and 80% by weight of PVME, with the remainder consisting of one of the polystyrenes, were prepared by spin coating a 2% w/w solution of the blend in toluene onto aluminum substrates spun at 1000 rpm for 40 s. The spin-coated

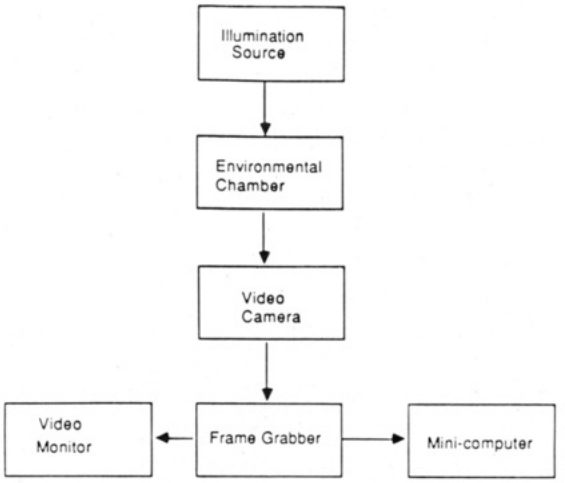

Figure 1. Block diagram of the automated pendant drop apparatus.

specimens were dried on the substrates for 2 days in a vacuum and were subsequently annealed for 2 weeks at temperatures in the range 50–80 °C, depending on the composition. Specimens for pendant drop measurements of surface tension were prepared by dissolving the blended materials in toluene and drying under vacuum for 1 week at 80 °C.

Surface Tension Measurements. Surface tensions of the homopolymers and blends were evaluated as a function of blend composition and temperature by using a pendant drop technique. The apparatus is shown schematically in Figure 1.

Drops of the blends and homopolymers were formed at elevated temperatures (ca. 100–170 °C) by using a Drummond positive displacement syringe with a glass capillary tip. Drops were formed inside a quartz cuvette that was placed in a Rame–Hart environmental chamber equipped with provisions for temperature control (±1 °C). All measurements were carried out under argon atmosphere. The optical system consisted of a Questar M1 microscope coupled to an NEC TI-22A CCD camera. The optics were focused by optimizing the video image of a reticle containing a finely ruled grid that was placed at the drop location. The reticle also provided a direct calibration of both the vertical and horizontal magnification factors inherent to the optics and camera system. The signal from the video camera was fed to a Tecmar Video van Gogh board that performed the frame grabbing and image digitization. Drop shape analysis was accomplished with a robust shape analysis algorithm.[40]

Estimation of the surface tension by the pendant drop technique requires a knowledge of the material density or specific volume. The specific volume relationship for PS4 (MW 3100) was obtained by interpolation of the data of Bender and Gaines.[41] The resultant temperature-dependent specific volume for PS4 is

$$\nu_{PS4}[\mathrm{cm}^3/\mathrm{g}] = 0.9310 + (6.0 \times 10^{-4})T[°\mathrm{C}] \quad (2)$$

A similar relationship for PVME was taken as[42]

$$\nu_{PVME}[\mathrm{cm}^3/\mathrm{g}] = 0.9709 + (5.92 \times 10^{-4})(T[°\mathrm{C}] - 25) \quad (3)$$

Blend densities were calculated from these expressions by assuming no volume change upon mixing. The densities of PS/PVME blends do exhibit a small positive deviation from additivity.[43] The constant-volume assumption therefore yields a density that is in error by approximately 1–2%. The precision in the surface tension measurements is ±0.5 dyn/cm.

XPS Instrumentation. XPS spectra were recorded with a modified AEI (Kratos) ES200B photoelectron spectrometer fitted with a Physical Electronics 04-151 achromatic Al $K\alpha_{12}$ source ($h\nu$ = 1486.7 eV). Typical operating conditions were as follows: X-ray source 10 KV, 60 mA, pressure in the source chamber $2–4 \times 10^{-8}$ Torr, and pressure in the analyzer chamber 6×10^{-7} Torr. The electron energy analyzer was operated by a PDP 11/23 computer in the fixed retarding ratio mode (for molecular weight studies) or fixed analyzer transmission mode (for angle-dependent experiments) through four 18-bit digital-to-analog converters (Analog Devices) and a data acquisition software package. The typical number of scans for each spectrum was four–eight. Under the experimental conditions employed, the $Ag_{3d\,5/2}$ peak at 386.27 eV binding energy had a full width at half maximum (fwhm) of 1.15 eV. Both PS and PVME contain hydrogen carbon, and therefore the binding energy of the C_{1s} signal at 285.0 eV was used as an internal calibration of the absolute binding energy scale.

Angular-dependent XPS measurements were carried out by rotating the samples relative to the fixed analyzer position by an angle θ, designated as the take-off angle between the sample normal and the entrance slit in the analyzer. The effective sampling depth is decreased by increasing the electron take-off angle.

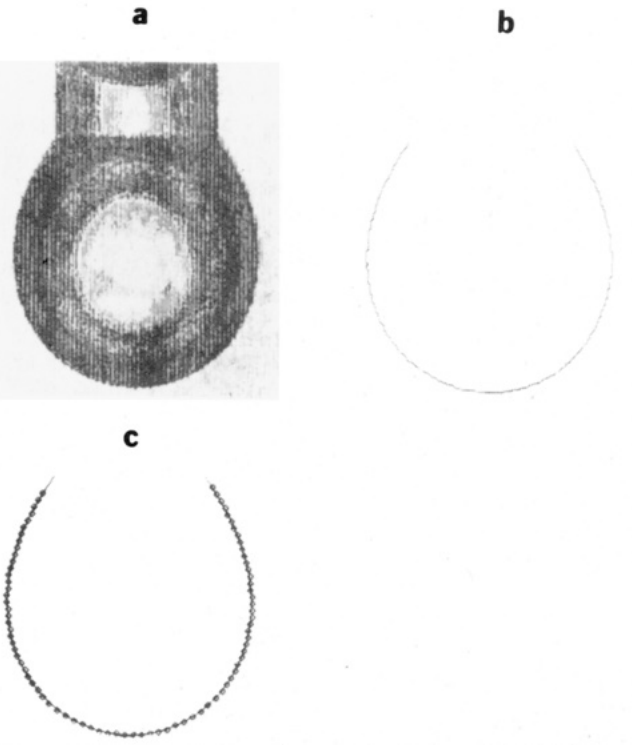

Figure 2. Pendant drop profile analysis of 95/05 w/w PS/PVME blend: (a) digitized image; (b) drop profile obtained by global thresholding; (c) theoretical profile from robust shape comparison (line), experimental profile (diamonds).

Analysis and Results

Surface Tension. Surface tensions of miscible blends of PS and PVME and the parent homopolymers were determined by digital image analysis of axisymmetric pendant fluid drops. A typical drop image is shown in Figure 2a. The theoretical profile of the drop is governed by a balance between gravitational forces and surface tension as expressed by the dimensionless Bashforth–Adams equations[44]

$$\begin{aligned} d\phi/dS &= 2/\beta + Z - (\sin\phi)/X \\ dX/dS &= \cos\phi \\ dZ/dS &= \sin\phi \end{aligned} \quad (4)$$

with boundary conditions

$$X(0) = 0, \quad Z(0) = 0, \quad d\phi/dS = 1/\beta, \quad \phi(0) = 0 \quad (5)$$

The dimensionless spatial coordinates are defined as $X \equiv xc^{1/2}$, $Z \equiv zc^{1/2}$, where x and z are the real Cartesian coordinates defining the drop profile, and $c^{1/2}$ is the scale or magnification factor defined as

$$c^{1/2} = \Delta\rho g/\gamma \quad (6)$$

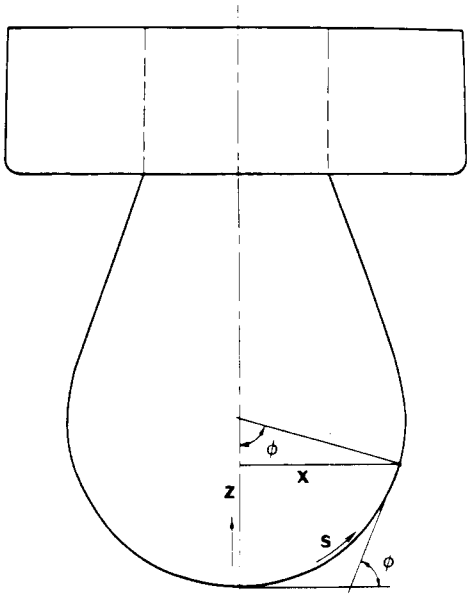

Figure 3. Pendant drop geometry.

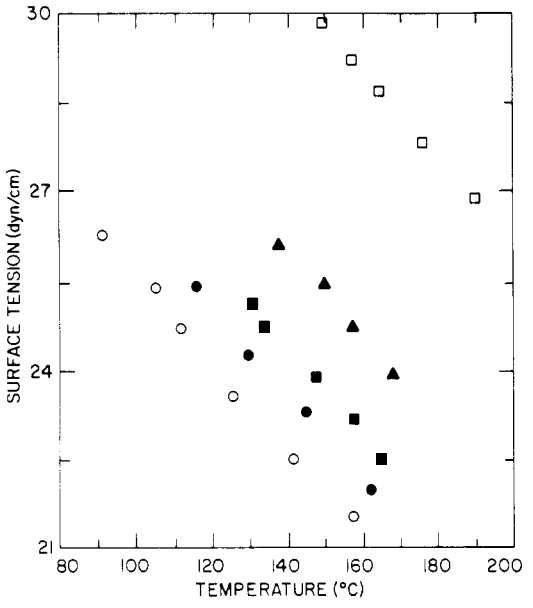

Figure 4. Surface tension of miscible blends of PS (3100), PVME homopolymers and blends: PVME homopolymer (open circles); PS/PVME 50/50 w/w (filled circles); PS/PVME 80/20 w/w (filled squares); PS/PVME 95/05 w/w (filled triangles); PS (3100) homopolymer (open squares).

The density difference across the interface is $\Delta\rho$, g is the gravitational constant, and γ is the surface tension. The dimensionless shape factor is taken as $\beta = bc^{1/2}$, while the dimensionless arc length is defined as $S = sc^{1/2}$, where b and s are the radius of curvature at the drop apex and the arc length, respectively. The relationships of these variables and the angle ϕ to the drop profile are illustrated in Figure 3.

The regression of the theoretical profile upon the experimental profile involves an optimization in five variables: x and z translations; a rotation of the camera axis with respect to the gravitational field; a magnification factor, $c^{1/2}$; and the shape parameter β. This regression was performed by using a robust shape comparison algorithm.[40] The result of edge detection by global thresholding is illustrated in Figure 2b. The final comparison of this experimental profile with the theoretical profile resulting from solution of eq 4–6 is shown in Figure 2c.

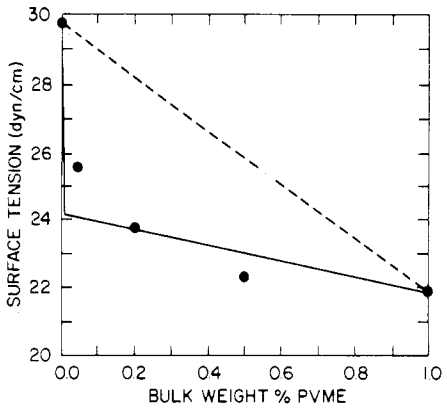

Figure 5. Surface tension of PS (3100)/PVME at 150 °C as a function of bulk weight percent PVME. Solid line is the monolayer theory[22] prediction with $\chi = 0$ and $a/kT = 0.49$ (dyn/cm)$^{-1}$. Dashed line is the expected result in the absence of preferential surface adsorption.

Table II
Surface Compositions from Surface Tension Data (150 °C)

wt fraction PVME (bulk)	wt fraction PVME (surf.)	surf. fraction PVME (f_{PVME})	distr coeff (K_{PVME})
0.05	0.567	0.573	11.3
0.20	0.769	0.773	3.8
0.50	0.933	0.935	1.9

Details pertaining to the shape analysis are given elsewhere.[40]

The pendant drop technique has been used to determine the composition and temperature dependence of the surface tension for binary miscible blends of PVME (MW 99 000) and PS4 (MW 3100). The results are presented in Figures 4 and 5. The surface tensions of the blends are effectively linear in temperature (Figure 4), as has been observed for pure homopolymers,[6] and show a temperature coefficient of $d\gamma/dT \sim -0.075$ dyn/(cm K).

The composition series (Figure 5) demonstrates that there is a considerable surface excess of PVME in the blends. This is particularly notable in the 50/50 w/w blend where the observed surface tensions correspond closely to the values for pure PVME homopolymer. The driving force for preferential surface adsorption of PVME is its lower surface tension (21.9 dyn/cm at 150 °C) compared to that of PS4 (29.7 dyn/cm at 150 °C).

If the surface tension of the blend is assumed to be proportional to the fractional surface coverage of each constituent, the surface fraction PVME can be estimated as

$$f_{PVME} = (\gamma_{blend} - \gamma_{PS})/(\gamma_{PVME} - \gamma_{PS}) \quad (7)$$

It follows that the weight fraction of PVME at the surface is

$$\omega_{PVME} = f_{PVME}\rho_{PVME}/[f_{PVME}\rho_{PVME} + (1 - f_{PVME})\rho_{PS}] \quad (8)$$

where the densities are given by (2) and (3). The relative enrichment can be described through a distribution coefficient for PVME defined as

$$K_{PVME} = (\omega_S/\omega_B)_{PVME} \quad (9)$$

where ω_S and ω_B are the surface and bulk weight fractions of PVME, respectively. The results of these calculations (Table II) indicate strong adsorption of PVME at the surface. These data show clearly that the relative enrichment is inversely related to the bulk PVME content.

The surface tension behavior of polymer solutions has been the subject of extensive theoretical treatment. Particular approaches that have formed the bases of much

Table III
Characteristics of XPS Core Levels for PS and PVME

	C_{1s} (hydrogen)		C_{1s} (oxygen)		C_{1s} ($\pi \rightarrow \pi^*$)	O_{1s}	
	BE[a]	fwhm[b]	BE	fwhm	BE	BE	fwhm
PS	285.0	1.40 ± 0.05			291.6 ± 0.1		
PVME	285.0	1.40 ± 0.05	286.6 ± 0.1	1.48 ± 0.05		533.2 ± 0.2	1.50 ± 0.05

[a] BE = binding energy in eV. [b] fwhm = full width at half-maximum in electronvolts.

of this effort are the parallel-layer model developed by Prigogine and co-workers[3] and extended to polymers by Gaines[22] et al. and the generalized square gradient theory popularized by Cahn[45] and adopted in many subsequent studies.[25,26,46]

For the case of surface tensions of polymers in solution with an attractive surface (i.e., the polymer is preferentially adsorbed at the air–solution interface) both approaches lead to an expression of the form

$$\gamma - \gamma_0 = K_1 + K_2\phi_B{}^m \tag{10}$$

where γ_0 is the surface tension of pure solvent, and ϕ_B is the bulk volume fraction of polymer in the solution. The constants K_1 and K_2 are dependent upon the local solute–interface interaction energy per unit surface area. The mean-field theories[25,26] yield a prediction of $m = 1$, while the monolayer theory prediction is variable depending on the relative size of the constituents and the interaction parameter. Scaling theory[47] also predicts behavior represented by eq 10; however, in the attractive case the exponent, m, is equal to 1.25.

The experimental data (Figure 5) correspond qualitatively to the functional form given by eq 10. An abrupt initial decrease in surface tension is observed, followed by a further decrease as the PVME concentration is increased. The concentration dependence is not linear as predicted by the mean-field theories; however, the data points are too few to establish whether they follow any particular power law dependence as given by (10). In addition, these theories were developed for polymer solutions and are not completely applicable for polymer blends.

The concentration dependence of surface tension is also predicted by the parallel-layer model.[3,22,24] This approach assumes that the surface contains a monolayer of material in equilibrium with the bulk phase. Although physically unappealing, the theory has produced predictions that are in agreement with more sophisticated theories for polymer solutions.[46] In applying the theory, we assume that polystyrene is the solvent. In the case of polymer blends,[48] the ratio of molar volumes (i.e., r in ref 22) is taken as 15.5, and the lattice parameter a is set to $(V_{PS}/N_0)^{2/3}$, where V_{PS} is the molar volume of polystyrene and N_0 is Avogadro's number. Since the Flory–Huggins expressions for free energy is employed in the theoretical development, only nonnegative values of the interaction parameter, χ, are appropriate. The interaction parameters for PVME/PS blends in the miscible state are negative;[33,35,36] however, the magnitude is small (ca. -1×10^{-4}), and we assume the mixture to be athermal (i.e., $\chi = 0$). The qualitative correspondence between the monolayer theory and experiment is excellent, as seen in Figure 5.

Proper account of the concentration dependence of surface tensions for our data would require an extension of the solution theories that would be appropriate for polymer blends. The framework for such a treatment has been presented by Poser and Sanchez[46] using the generalized square gradient approach. This treatment can account for the nonlinear concentration dependence of surface tension for polymer solutions, but its application to miscible blends involves specification of two parameters

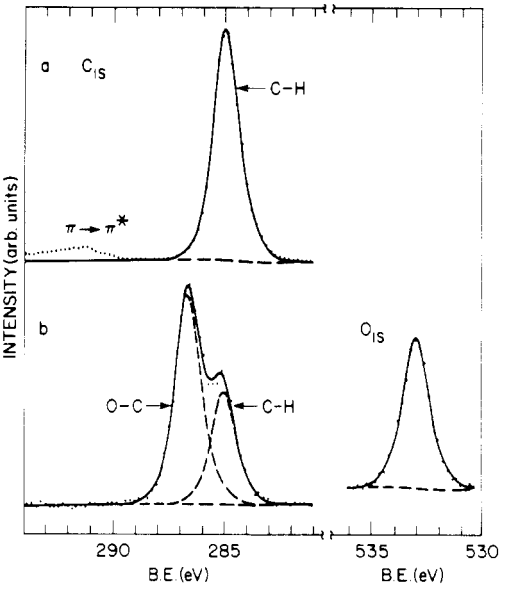

Figure 6. C_{1s} and O_{1s} spectra for polystyrene and poly(vinyl methyl ether) homopolymers.

associated with mixing rules for the polymer–polymer interaction energy and specific volume. In principle, values for these parameters may be determined experimentally, allowing direct calculation of the surface tension of the blend. The feasibility of this approach is currently under consideration.

X-ray Photoelectron Spectroscopy. Quantitative analysis of the XPS data focuses on resolution of the C_{1s} spectra for the PS/PVME blends. The C_{1s} spectra for pure PVME (Figure 6a) is a doublet containing contributions from carbon–oxygen (at 286.6 eV) and carbon–hydrogen bonds (at 285 eV). The C_{1s} spectra for PS (Figure 6b) shows only a singlet carbon–hydrogen peak and a small satellite peak at 291.6 eV due to a π to π^* shake-up transition.[49] Characteristics of the homopolymer core level spectra are given in Table III.

Typical data for the miscible blends (Figure 7) exhibit doublets as a result of superposition of the two homopolymer spectra. The surface composition can be extracted from these spectra by resolving the two contributions and calculating the integrated area under each peak.

The integrated intensity I_i of a core-electron photoemission spectrum is given by[50]

$$I_i \propto N_i S_i \tag{11}$$

where N_i is the average number of atoms per unit sampling volume and S_i is the sensitivity factor. The sensitivity factor for carbon atoms in two distinct chemical environments is approximately identical, and therefore the intensity ratio is equal to the average atomic ratio of the two types of carbon atoms. The area intensity ratio of oxygen to hydrogen carbon, calculated by a peak fitting program, can be expressed as

$$\frac{I_{CO}}{I_{CH}} = \frac{2\omega}{M_V} \Big/ \left(\frac{\omega}{M_V} + \frac{8(1-\omega)}{M_S} \right) \tag{12}$$

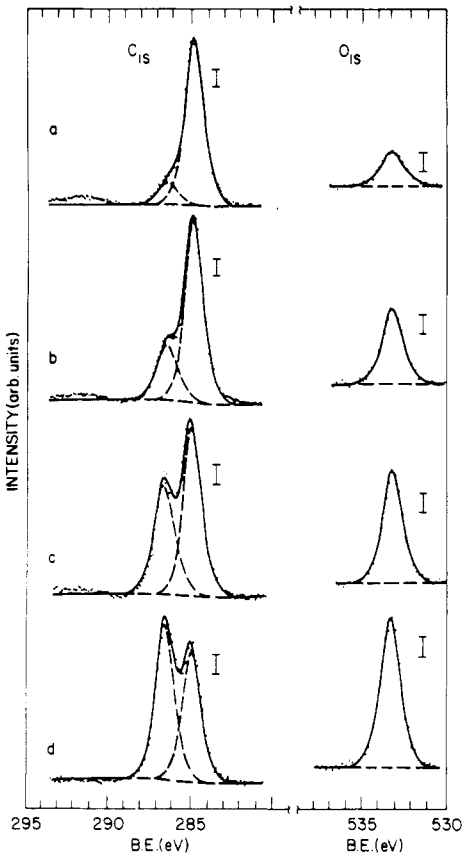

Figure 7. C_{1s} and O_{1s} core level spectra for the miscible PS/PVME blends: (a) 95/05; (b) 80/20; (c) 50/50; (d) 20/80. Dashed lines indicate the individual peak contributions obtained from curve resolution. The brackets denote a signal of 100 counts/s.

where ω is the average weight fraction of PVME within the sampling depth. M_S and M_V are the molecular weights of the styrene and vinyl methyl ether repeat units, respectively.

The photoemission peaks in the raw, uncorrected spectra are superimposed over an inelastic scattering background. This background was estimated according to the method used by Proctor and Sherwood.[51] After background subtraction, resolution of the C_{1s} spectra into the C–O and C–H contributions was accomplished by fitting a combination of Gaussian and Lorentzian intensity functions to the data. These distributions are defined by the peak maximum positions, full width at half maximum values, peak maximum intensities, and percentage of Gaussian. In practice, the peak regression for blend specimens was carried out by manually fixing the positions of the C–O and C–H peaks and the fwhm of the C–O peak and subsequently calculating the fwhm of the C–H peak and the peak intensities by a nonlinear regression algorithm. Initial values for these parameters were obtained by analysis of the pure PS and PVME homopolymers. The best fit was obtained by manual iteration on this procedure and was determined to be that set of parameters that gave the minimum sum of squared residuals normalized by the total sum of squares. The statistical error inherent to the regression analysis leads to errors of ±3–5 wt % in the surface composition. This error is largest for grazing take-off angles.

As the result of a relatively high source chamber pressure, $\sim 10^{-8}$ Torr, a nonnegligible hydrocarbon contamination layer is continuously deposited on the specimen during the experiment. The hydrocarbon contamination gives rise to a small contribution to the C_{1s} spectrum at 285.0 eV. Hydrocarbon contamination is a universal

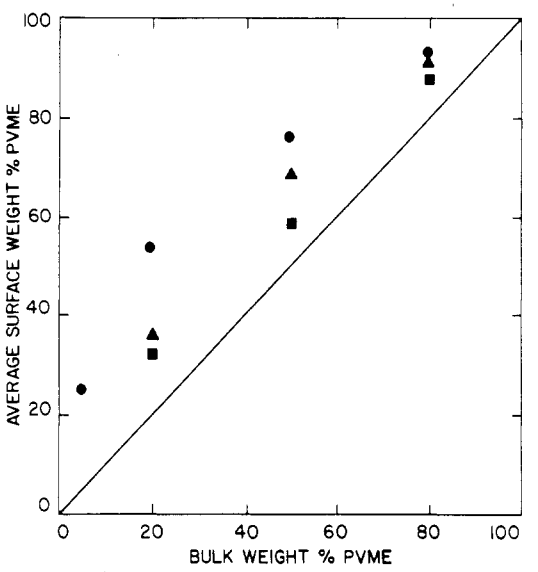

Figure 8. Average surface weight percent versus bulk weight percent PVME: PS constituent of molecular weight 127 000 (circles); PS molecular weight 3100 (triangles); PS molecular weight 1200 (squares).

Table IV
XPS Distribution Coefficients as a Function of Blend Composition and Polystyrene Molecular Weight

wt fraction PVME (bulk)	distr coeff		
	M_{PS} 127 000	M_{PS} 3100	M_{PS} 1200
5	5		
20	2.66	1.72	1.6
50	1.53	1.37	1.17
80	1.16	1.14	1.1

Table V
Composition Gradient Parameters for Blends of PVME (M_w 99 000) and PS (M_w 127 000)

wt fraction PVME	ξ, nm	α	ϕ (z = 0)
0.05	5.0	0.28	0.65
0.20	3.5	0.51	0.90
0.50	7.0	0.89	0.98

phenomenon in XPS experiments that has been attributed to the heating of the X-ray source and the presence of diffusion pump oil at finite pressure.[52] While the atomic ratio of oxygen carbon to hydrogen carbon is exactly 2:1 for pure PVME, the measured ratio is found to be 2:(1 + x) where x is positive and a function of time, t, and electron take-off angle, θ. $x(\theta,t)$ was determined from measurements on pure PVME and was assumed to be identical for all blend samples. With this assumption the contribution of the hydrocarbon contamination was accounted for in the analysis.

Composition Dependence. The surface enrichment of PVME is dependent on the molecular weights of the blend constituents and the overall blend composition. This is illustrated in Figure 8, where the "average" surface composition is given as a function of the overall blend composition. The "average" surface concentration reflects the total of all material residing in the sampling depth (~70 Å). The relative amount of surface enrichment is represented by the distribution coefficients (see eq 9) given in Table IV.

In general, the trends with changing composition are similar to those seen in the surface tension data. The magnitudes of the XPS distribution coefficients, however, are smaller than those from the surface tension analysis. This results primarily from the fact that the XPS measurement samples the composition distribution integrated

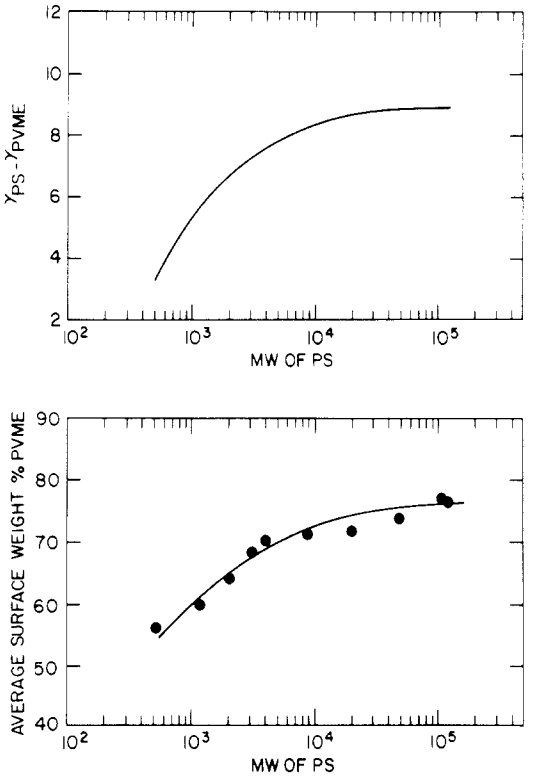

Figure 9. (a) Surface tension difference between PS and PVME homopolymers versus molecular weight of PS. (b) Average surface weight percent PVME obtained from XPS versus molecular weight of PS.

over a depth of ca. 70 Å, while the surface tension data more appropriately reflect the composition of the outermost surface layer. In addition, the XPS measurements were carried out at room temperature, while the surface tension data were collected at elevated temperatures.

Molecular Weight Effects. At fixed composition, the surface enrichment of PVME becomes more dominant as the PS molecular weight increases. This behavior is a direct consequence of the molecular weight dependence of the PS surface energy. It is well-known that homopolymer surface tension increases as the chain length is increased.[6] The driving force for PVME surface enrichment (i.e., $\gamma_{PS} - \gamma_{PVME}$) therefore becomes larger as the PS molecular weight is increased.

LeGrand and Gaines[53] have shown that the molecular weight dependence of homopolymer surface tension follows an empirical expression of the form

$$\gamma = \gamma_\infty - K_e/M_n^{2/3} \tag{13}$$

where M_n is the number average molecular weight. For polystyrene at 177 °C, values of the empirical constant, K_e, and surface tension at infinite molecular weight, γ_∞, have been reported as 372.7 dyn dalton$^{2/3}$/cm and 29.97 dyn/cm, respectively.[54]

The relationship between the driving force for surface adsorption and the resultant surface composition is illustrated in Figure 9. The blends contain PVME of fixed molecular weight (MW 99 000, $M_w/M_n \simeq 2$) with PS of varying molecular weight. The compositions of these blends are all identical at 50% bulk weight of PS. Surface compositions were calculated from XPS spectra obtained with the take-off angle normal to the surface and analyzed according to eq 12. The theoretical driving force, $\gamma_{PS} - \gamma_{PVME}$, was estimated by subtracting the measured surface tension for PVME (at 177 °C) from the empirical expression (eq 13) for PS surface tension.

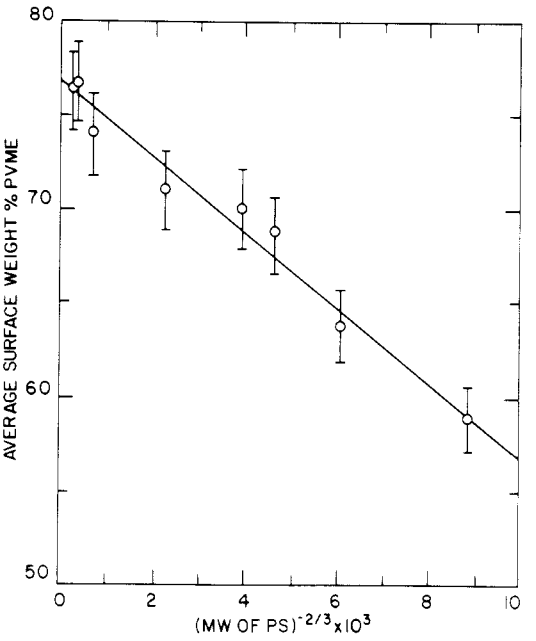

Figure 10. Average surface weight percent PVME obtained from XPS versus (molecular weight of PS)$^{-2/3}$.

Since $d\gamma/dT$ is essentially identical for the blends and homopolymers, the surface tension difference will be insensitive to the temperature. Thus, although the XPS spectra were obtained at room temperature, the calculated surface tension difference (at 177 °C) should still be an appropriate value to use for comparison. The close correspondence between surface energy difference and surface composition suggests that the molecular weight dependence of surface composition should follow a functional form similar to that for surface tension (i.e., eq 13). That is, for fixed PVME molecular weight, $\gamma_{PS} - \gamma_{PVME}$ is proportional to $M_n^{-2/3}$. It then follows that the average surface composition should exhibit the same molecular weight dependence. The empirical $M_n^{-2/3}$ molecular weight dependence is borne out by the XPS data on the 50% bulk weight PS blends as illustrated in Figure 10. A least-squares fit of this data yields an empirical expression for the surface weight fraction of PS of form

$$\omega_{PS} = 23.1 + (2.03 \times 10^3)/M_n^{2/3} \tag{14}$$

There was some concern during the measurements that the use of polydisperse poly(vinyl methyl ether) ($M_w/M_n \simeq 2$) could complicate the behavior as a result of surface fractionation of low molecular weight PVME molecules. The correspondence between surface energy difference and surface composition (Figure 9) suggests that fractionation of species according to molecular weight does not occur. Surface analyses of bimodal molecular weight blends of polystyrenes by secondary ion mass spectrometry[55] and by surface tension analysis[16] also failed to document any surface fractionation according to molecular weight.

Surface Composition Profiles. The surface concentration gradient is amenable to characterization by XPS experiments. Concentration depth profiling can be accomplished by changing the photoelectron take-off angle to the analyzer[56,57] as depicted schematically in Figure 11. The sampling depth of XPS is limited by the effective mean free path for electrons escaping from the surface. At take-off normal to the surface, the effective sampling depth is a maximum, given approximately by $z \simeq 3\lambda$, where λ is the mean free path. When nonnormal take-off angles are used, the sampling depth decreases according to

$$Z \simeq 3\lambda \cos\theta \tag{15}$$

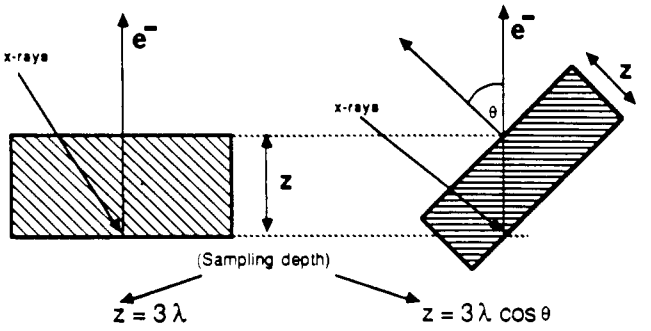

Figure 11. Schematic diagram of angle-dependent XPS experiment for depth profiling studies: z = effective sampling depth; λ = electron mean free path.

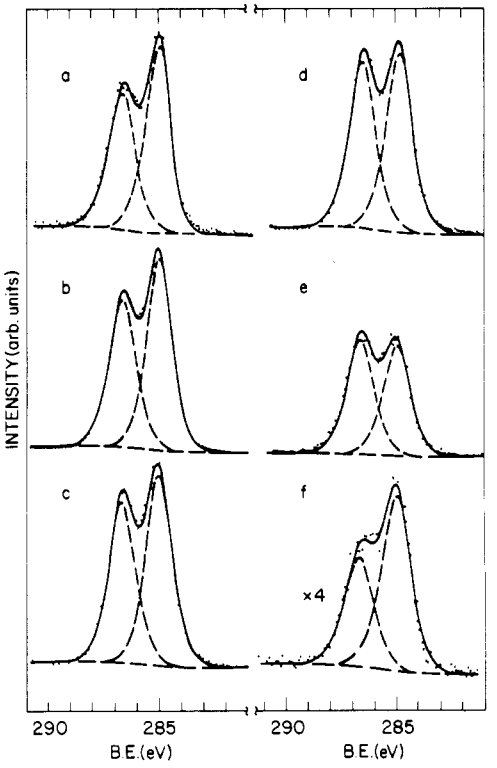

Figure 12. C_{1s} XPS spectra as a function of take off angle, θ, for the miscible 50/50 w/w PS/PVME blend: (a) 0°; (b) 30°; (c) 50°; (d) 60°; (e) 70°; (f) 80°. Dashed lines are the results of curve resolution.

where θ is the angle between the sample normal and the emitted electron path to the analyzer as shown in Figure 11. Approximately 95% of the photoelectrons detected in the experiment emanate from the sampling depth defined in this fashion.

Accurate knowledge of the electron mean free path is vital to the quantitative success of XPS depth profiling; however, there is considerable discrepancy in the literature values for λ. Electron mean free paths for polymers have been discussed in detail by Clark.[58] Following their conclusions, we have chosen to use the value $\lambda = 23 \pm 3$ Å. This value was also obtained by Szajman et al.[59]

Hydrocarbon contamination and surface roughness[60] also lead to uncertainty in the value of z, especially at grazing angles. The effects of hydrocarbon contamination are minimized by using fresh samples for every pair of take-off angles and by subtracting a hydrocarbon signal $x(\theta,t)$ estimated from experiments on pure PVME as discussed earlier in this paper. Even with these precautions, the errors in the experimental integrated surface compositions for small z are considerable. Application of the substrate overlayer model to these data furnishes a maximum thickness of 3 Å for the contamination layer.

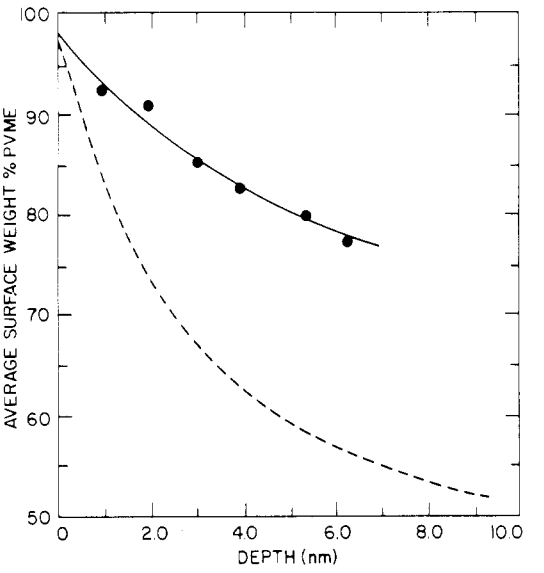

Figure 13. Integral surface composition profile of 50/50 w/w miscible PS/PVME blend determined by angle-dependent XPS (circles). Solid line is the fit obtained by using $\coth^2 [(z/\xi) + \alpha]$ profile in expression 16, where $\xi = 7.0$ nm and $\alpha = 0.89$. Dashed line is the $\coth^2 [(z/\xi) + \alpha]$ profile.

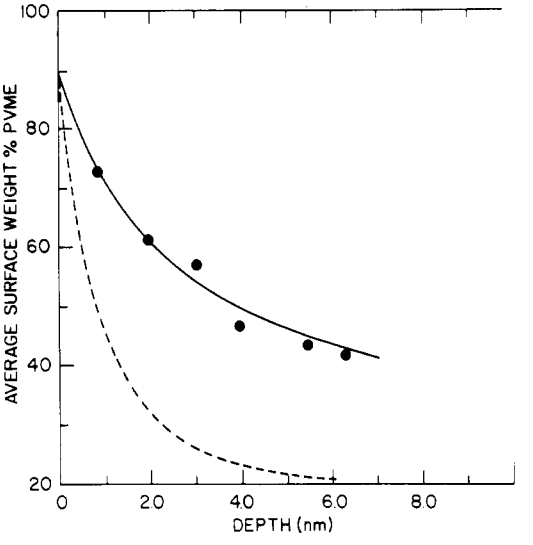

Figure 14. Integral surface composition profile of 80/20 w/w miscible PS/PVME blend determined by angle-dependent XPS (circles). Solid line is the fit obtained by using $\coth^2 [(z/\xi) + \alpha]$ profile in expression 16, where $\xi = 3.5$ nm and $\alpha = 0.51$. Dashed line is the $\coth^2 [(z/\xi) + \alpha]$ profile.

Representative angle-dependent C_{1s} core-level spectra for a 50/50 PS/PVME blend are shown in Figure 12. Analysis of this data according to eq 12 gives the corrected average surface composition as a function of effective sampling depth as shown in Figure 13. This profile is in good agreement with data on a similar specimen reported by Pan and Prest.[31] The PVME surface concentration increases smoothly from the bulk value to attain a value of ca. 98% in the outermost surface layer. Similar behavior is observed for 5/95 and 20/80 blends (Figure 14 and 15).

The XPS depth profile data do not furnish a direct measurement of the surface composition gradient. Due to the nature of the XPS experiment, the surface composition measured is actually an integral value of the composition averaged over the sampling depth. For the core-level spectra of a particular atomic species, the pho-

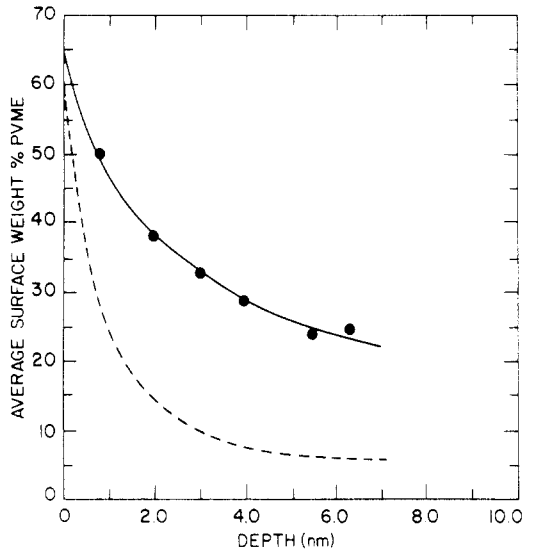

Figure 15. Integral surface composition profile of 80/20 w/w miscible PS/PVME blend determined by angle-dependent XPS (circles). Solid line is the fit obtained by using $\coth^2 [(z/\xi) + \alpha]$ profile in expression 16, where $\xi = 5.0$ nm and $\alpha = 0.28$. Dashed line is the $\coth^2 [(z/\xi) + \alpha]$ profile.

toelectron intensity for core-level j at take-off angle θ may be expressed as[56]

$$I_j(\theta) \propto \int_0^\infty n_j(z) \exp[-z(\lambda_j \cos \theta)]\, dz \qquad (16)$$

where $n_j(z)$ represents the atomic composition depth profile for the species of interest (e.g., C–O or C–H in the present case).

For the PVME/PS blends, we have calculated the average surface weight fractions as a function of sampling depth through application of eq 12 to angle-dependent XPS spectra. A model for the concentration gradient, $n_j(z)$, is required to accomplish this, whereupon the intensities $I_j(\theta)$ can be determined by (16) and the average surface composition profile $\omega(z)$ can be calculated through eq 12. This profile can be compared directly to an experimental profile such as is given in Figures 13–15.

Some of the theories that were discussed previously for surface tension of polymer solutions also make predictions for the concentration gradient at the air–solution interface. For an attractive interface, the predicted concentration profile is[25]

$$\phi(z) = \phi_B \coth^2 [(z/\xi) + \alpha] \qquad (17)$$

where ξ is the Edwards correlation length[61,62] and α is a constant related to the surface density.

The experimental integrated profiles are modeled by using this profile in expression 16. The results are shown in Figures 13–15. For all cases studied, the concentration profile predicted by the mean-field solution theories compares well with the experimental data for the miscible blends. The resultant fit parameters are summarized in Table V.

The concentration dependence of the screening length, ξ, in polymer solutions is predicted by several theories[61-64] and is a function of the concentration regime of the phase diagram. Unfortunately, the data in Table V do not cover a large concentration regime and are not of sufficient accuracy or precision to examine the correspondence with the theoretical predictions.

The magnitude of the screening lengths are reasonable, however. The theoretical screening length is bounded by the PVME radius of gyration (for low concentrations) and the statistical segment length of PVME (for bulk PVME). Values of these limits for similar blends have been reported as 9.7 nm[65] and 0.35 nm,[66] respectively. The experimental screening lengths do fall within these limits.

Extensions of the Sanchez–Poser[46] treatment could again be applied to model the concentration profiles; however, we do not have sufficient experimental data to properly accomplish this at the present time.

Summary

The surface character of miscible PVME/PS blends has been examined as a function of the overall blend compositions, the constituent molecular weights, and the temperature. Surface tension data and XPS analysis demonstrate substantial surface enrichment of PVME for all of the blends examined and under all tested conditions. The PVME exhibits strong surfactant behavior, causing a dramatic reduction in surface tension when even small quantities are added. By comparison of XPS and surface tension data, we show a direct correspondence between the driving force for surface segregation (i.e., the surface energy difference between PS and PVME) and the resultant surface composition. This relationship is emphasized by the results of XPS measurements on the molecular weight dependence of the surface composition. An empirical $M_n^{-2/3}$ power law dependence of surface composition is observed, reflecting clearly the empirical $M_n^{-2/3}$ dependence of the surface energy difference. Surface composition gradients determined by angle-dependent XPS experiments are well represented by the profiles predicted by mean-field theories of polymer solutions. The experimental profiles indicate that the PVME content of the outermost surface layer increases with the bulk PVME content and attains values as high as 98% for certain blends. The combination of X-ray photoelectron spectroscopy for determination of surface structure and pendant drop measurements of surface tension for characterization of surface thermodynamics constitutes an extremely powerful means for the investigation of the surface properties of polymeric materials.

Acknowledgment. Partial support of this research (J.T.K. and Q.S.B.) was supported by a joint research grant from the Army Research Office and the Polymer Program of the National Science Foundation (DMR No. 8504727). D.H.P. acknowledges Xerox's continuing support for the industry–university joint research project.

Registry No. PS, 9003-53-6; PVME, 9003-09-2.

References and Notes

(1) Blakely, J. M. In *Chemistry and Physics of Solid Surfaces*; Vanselow, R., Eds.; CRC Press: Boca Raton, FL, 1979; Vol. 2.
(2) Carey, B. S.; Scriven, L. E.; Davis, H. T. *AICHE J.* **1980**, *26*, 705.
(3) Defay, R.; Prigogine, I.; Bellemans, A. *Surface Tension and Adsorption*; Wiley: New York, 1951.
(4) Thomas, H. R.; O'Malley, J. J. *Macromolecules* **1981**, *14*, 1316.
(5) Schmitt, R. L.; Gardella, J. A., Jr.; Salvati, L. *Macromolecules* **1986**, *19*, 648.
(6) Wu, S. *Polymer Interface and Adhesion*; Dekker: New York, 1982.
(7) Rastogi, A. K.; St. Pierre, L. E. *J. Colloid Interface Sci.* **1969**, *31*, 168.
(8) Owen, M. J.; Kendrick, J. C. *Macromolecules* **1970**, *3*, 458.
(9) Clark, D. T.; Peeling, J.; O'Malley, J. J. *J. Polym. Sci. Polym. Chem. Ed.* **1976**, *14*, 543.
(10) Thomas, H. R.; O'Malley, J. J. *Macromolecules* **1979**, *12*, 323.
(11) O'Malley, J. J.; Thomas, H. R.; Lee, G. M. *Macrmolecules* **1979**, *12*, 966.
(12) Schmitt, R. L.; Gardella, J. A., Jr.; Magill, J. H.; Salvati, L., Jr.; Chin, R. L. *Macromolecules* **1985**, *18*, 2675.
(13) McGrath, J. E.; Dwight, D. W.; Riffle, J. S.; Davidson, T. F.; Webster, D. C.; Vishwanathan, R. *Polym. Prepr. (Am. Chem. Soc., Div. Polym. Chem.)* **1979**, *20* (2), 528.

(14) Gervais, M.; Douy, R.; Gallot, B.; Erre, R. *Polymer* **1986**, *27*, 1513.
(15) Kugo, K.; Hata, Y.; Hayashi, T.; Nakajima, A. *Polym. J.* **1982**, *14*, 401.
(16) Gaines, G. L., Jr.; Bender, G. W. *Macromolecules* **1972**, *5*, 82.
(17) Yamashita, Y. *J. Macromol. Sci., Chem.* **1979**, *A13*, 401.
(18) Owens, D. K. *J. Appl. Polym. Sci.* **1970**, *14*, 185.
(19) Kendrick, T. C.; Kingston, B. M.; Lloyd, N. C.; Owen, M. J. *J. Colloid Interface Sci.* **1967**, *24*, 135.
(20) Gaines, G. L., Jr. *Macromolecules* **1981**, *14*, 1366.
(21) Fredrickson, G. H. *Macromolecules* **1987**, *20*, 2535.
(22) Gaines, G. L., Jr. *J. Phys. Chem.* **1969**, *73*, 3143.
(23) Gaines, G. L., Jr. *J. Polym. Sci. Part A-2* **1969**, *7*, 1379.
(24) Siow, K. S.; Patterson, D. *J. Phys. Chem.* **1973**, *74*, 356.
(25) Ober, R.; Paz, L.; Taupin, C.; Pincus, P.; Boileua, S. *Macromolecules* **1983**, *16*, 50.
(26) DiMeglio, J. M.; Ober, R.; Paz, L.; Taupin, C.; Pincus, P.; Boileau, S. *J. Phys. (Les Ulis, Fr.)* **1983**, *44*, 1035.
(27) Koberstein, J. T. In *Encyclopedia of Polymer Science and Engineering*; Wiley: New York, 1987; Vol. 8, p 237.
(28) Busscher, H. J.; Hoogsteen, W.; Dijkema, L.; Sawatsky, G. A.; van Pelt, A. W. J.; de Jong, H. P.; Challa, G.; Arends, J. *Polym. Commun.* **1985**, *26*, 252.
(29) LeGrand, D. G.; Gaines, G. L., Jr. *J. Polym. Sci., Part C* **1971**, *34*, 45.
(30) Flory, P. J. *Principles of Polymer Chemistry*; Cornell University Press: Ithaca, NY, 1953.
(31) Pan, D. H.; Prest, M. W., Jr. *J. Appl. Phys.* **1985**, *58*, 15.
(32) McMaster, L. P. *Macromolecules* **1973**, *6*, 760.
(33) Nishi, T.; Wang, T. T.; Kwei, T. K. *Macromolecules* **1975**, *8*, 227.
(34) Kwei, T. K.; Wang, T. T. In *Polymer Blends*; Paul, D. R., Newman, S., Eds.; Academic: New York, 1978; Vol. 1.
(35) Hadziioannou, G.; Stein, R. *Macromolecules* **1984**, *17*, 567.
(36) Shiomi, T.; Kohno, K.; Yoneda, K.; Tomita, T.; Miya, M.; Imai, K. *Macrmolecules* **1985**, *18*, 414.
(37) Jelenic, T.; Kirste, R. G.; Oberthuer, R. C.; Schmitt-Streeker, S.; Schmitt, B. J. *Makromol. Chem.* **1984**, *12*, 185.
(38) Bhatia, Q. S.; Chen, J. K.; Koberstein, J. T.; Sohn, J. E.; Emerson, J. A. *J. Colloid Interface Sci.* **1985**, *106*, 352.
(39) Anastasiadis, S. H.; Chen, J. K.; Koberstein, J. T.; Sohn, J. E.; Emerson, J. A. *Polym. Eng. Sci.* **1986**, *26*, 1410.
(40) Anastasiadis, S. H.; Chen, J. K.; Koberstein, J. T.; Sohn, J. E.; Emerson, J. A.; Siegel, A. F. *J. Colloid Interface Sci.* **1987**, *119*, 55.
(41) Bender, G. W.; Gaines, G. L., Jr. *Macromolecules* **1970**, *3*, 128.
(42) Van Krevelen, D. W. *Properties of Polymers*; Elsevier: Amsterdam, 1976.
(43) Kwei, T. K.; Nishi, T.; Roberts, R. F. *Macromolecules* **1974**, *7*, 667.
(44) Hartland, S.; Hartley, R. W. *Axisymmetric Fluid-Liquid Interface*; Elsevier: Amsterdam, 1976.
(45) Cahn, J. W. *J. Chem. Phys.* **1977**, *66*, 3667.
(46) Poser, C. I.; Sanchez, I. C. *Macromolecules* **1981**, *14*, 361.
(47) de Gennes, P.-G. *Macromolecules* **1981**, *14*, 1637.
(48) Bhatia, Q. S. Ph.D. Thesis, Princeton University, 1987.
(49) Clark, D. T.; Dilks, A. *J. Polym. Sci., Polym. Chem. Ed.* **1976**, *14*, 533.
(50) Wagner, C. D.; Riggs, W. M.; Davis, L. E.; Moulder, J. F.; Muilenberg, J. E. *Handbook of X-ray Photoelectron Spectroscopy*, Perkin–Elmer Corp., 1979.
(51) Proctor, A.; Sherwood, P. M. A. *Anal. Chem.* **1982**, *54*, 13.
(52) Clark, D. T.; Thomas, H. R.; Dilks, A.; Shuttleworth, D. J. *Electron Spectrosc. Relat. Phenom.* **1971**, *10*, 435.
(53) LeGrand, D. G.; Gaines, G. L., Jr. *J. Colloid Interface Sci.* **1969**, *31*, 162.
(54) Wu, S. In *Polymer Blends*; Paul, D. R., Newman, S., Eds., Academic: New York, 1978.
(55) Goldblatt, R. D.; Scilla, G. J.; Park, J. M.; Johnson, J. N.; Huang, S. *J. Appl. Polym. Sci.*, in press.
(56) Fadley, C. S.; Bergström, S. A. L. *Phys. Lett. A* **1971**, *35a*, 375.
(57) Fadley, C. S. *Prog. Surf. Sci.* **1984**, *16*, 275.
(58) Clark, D. T.; Thomas, H. R. *J. Polym. Sci., Polym. Chem. Ed.* **1977**, *15*, 2843.
(59) Szajman, J.; Liesegang, J.; Jenkin, J. G.; Leckey, R. G. G. *J. Electron Spectrosc. Relat. Phenom.* **1978**, *14*, 247.
(60) Fadley, C. S.; Baird, R. J.; Sickhaus, W.; Novakov, T.; Bergström, S. A. L. *J. Electron Spectrosc.* **1974**, *4*, 93.
(61) Edwards, S. F. *Proc. Phys. Soc., London* **1966**, *88*, 265.
(62) Edwards, S. F.; Jeffers, E. F. *J. Chem. Soc., Faraday Trans. 2* **1979**, *75*, 1020.
(63) Daoud, M.; Jannink, G. *J. Phys. (Les. Ulis, Fr.)* **1975**, *37*, 973.
(64) Schaefer, D. W. *Polymer* **1984**, *25*, 387.
(65) Hashimoto et al., unpublished results quoted by Schichtel; Binder, *Macromolecules* **1987**, *20*, 1679.
(66) Schwan, D., et al. *J. Chem. Phys.*, in press.

Entanglement in Blends of Monodisperse Star and Linear Polystyrenes. 1. Dilute Blends

Hiroshi Watanabe,† Hirotsugu Yoshida, and Tadao Kotaka*

Department of Macromolecular Science, Faculty of Science, Osaka University, Toyonaka, Osaka 560, Japan. *Received October 1, 1987; Revised Manuscript Received January 19, 1988*

ABSTRACT: Viscoelastic properties of binary blends composed of narrow molecular weight distribution (MWD) 4-arm star polystyrenes (2-chain) of molecular weight (MW) M_2 and narrow MWD linear polystyrenes (1-chain) of M_1 were examined and compared with binary blends of narrow MWD linear polystyrenes of M_2 and M_1. In these blends, the volume fraction ϕ_2 of the 2-chain was kept small so that the 2-chains were entangling only with the matrix 1-chains but not with themselves. When the MW of the components of these dilute blends were such that $M_c < M_1 \ll M_2$, with M_c being the characteristic MW, the star 2-chain exhibited Rouse–Ham-like relaxation modes with the (weight average) relaxation time proportional to $\phi_2^0 M_1^3 M_2^2$ and the compliance proportional to $\phi_2^{-1} M_1^0 M_2$. Similar behavior was also found in the dilute blends of linear chains. These results suggest that the star as well as the high-MW linear (2-) chain in the dilute blend with $M_2 \gg M_1 > M_c$ may relax as the surrounding 1-chains diffuse away so that the 1–2 entanglement has become ineffective. In the framework of the generalized tube model, this relaxation mechanism corresponds to the *tube renewal* mode. The limiting ratio of M_2/M_1, for which these power laws are valid, is smaller for the star/linear chain blends than that for the linear chain blends. This is because the intrinsic relaxation time of the star 2-chain of M_2 is longer than that of the linear 2-chain of the same M_2, observed in the bulk states. Thus, the star 2-chain exhibits the Rouse–Ham modes more easily than the corresponding linear 2-chain in the same matrix 1-chains.

Introduction

Blends of narrow molecular weight distribution (MWD) polymers are simple but important model systems for examining the effects of *entanglement* on the relaxation behavior of condensed polymer systems.[1–11] Recently, several groups including ourselves studied viscoelastic[3–11] and diffusion[12–15] properties of binary blends of narrow MWD linear polymers of high and low MW. In such a blend the terminal relaxation modes of the high-MW chain (the test chain) are strongly affected by the lifetime of the

†On leave from the Department of Chemical Engineering and Materials Science, 151 Amundson Hall, University of Minnesota—Twin Cities, 421 Washington Ave. S.E., Minneapolis, MN 55455.

0024-9297/88/2221-2175$01.50/0